

Research Article

Flow-Through Portable Antivirus UV-C Optical Enclosures to be Used with Protective Masks

Ozgur Selimoglu 

Department of Energy Engineering, Faculty of Engineering, Ankara University, 06830 Golbasi, Ankara, Turkey

Correspondence should be addressed to Ozgur Selimoglu; selimogluozgur@gmail.com

Received 27 July 2021; Revised 16 October 2021; Accepted 26 October 2021; Published 11 November 2021

Academic Editor: Sulaiman W. Harun

Copyright © 2021 Ozgur Selimoglu. This is an open access article distributed under the Creative Commons Attribution License, which permits unrestricted use, distribution, and reproduction in any medium, provided the original work is properly cited.

UV-C light is an important disinfection tool against airborne viruses, while also being harmful if the light reaches the human skin. Body-attached reflective flow-through optical enclosures can be used for isolating the UV-C light from the user as well as elevating the irradiance level. In this study, we explain why air-sterilizing light enclosures are more effective than the expectations by introducing a dose multiplication factor of 4. As a result of omnidirectional illumination, air sterilization becomes more effective than surface disinfection if similar irradiance levels are measured from the enclosure wall. The methodology is explained by the design of a portable enclosure device primarily targeting the COVID-19 virus, and disinfection effectiveness better than 99.5% is demonstrated by biological tests.

1. Introduction

UV light is an important tool to sterilize air with low power consumption in a shorter time. UV-C radiation, ranging in wavelength from 200 to 280 nm (also referred to as UV germicidal irradiation or UVGI), is accepted as the most effective form of UV light for sterilization as the light in this wavelength range is strongly absorbed by nucleic acids [1]. Although DNA and RNA content can be different concerning the type of airborne virus, UV-C light is effective on both kinds of genetic material by altering the molecular bonds, and the replication ability of the virus is terminated.

Room-type systems are currently in use to neutralize viruses in indoor environments. Recently, many air conditioning systems are also utilized with UV-C light to supply sterilized air to buildings. There are many ongoing research studies around the world to make UV-C systems safe and efficient [2–8].

Besides the large building integrated type systems, portable and human-attached air disinfection devices can prevent airborne virus infection by sterilizing the air

supplied to the face masks. For travelers and office workers, portable air disinfecting UV-C devices can be very effective as they cannot control the air quality of the indoor environment that they have to share with other people.

To neutralize the airborne viruses in airflow, an extremely high dosage of UV light is necessary for a short time. A light dosage level that is effective on viruses is also dangerous to any living organism. High UV levels should not be used with the human presence. Trapping the high-level UV light into an enclosure while allowing airflow can be a solution. Highly reflective small enclosures can easily achieve high sterilization doses. The enclosure should permit the flow of air, while UV-C light should be kept inside the enclosure. A very little amount of light leakage is allowable for these systems as UV-C light is dangerous for humans and living organisms.

In literature, a patent application dated back to 1992 is encountered for portable UV-C applications. The concept is theoretically introduced, but no further information or publication is accessible about the idea. It is claimed that air breathed in by the user has been exposed to inbuilt UV

radiation, killing pathogens and viruses [9]. Sterilized air is supplied to the face mask via an air tube, as shown in Figure 1.

Encountered studies through the literature are related to mask decontamination which is related to the surface disinfection application [3–8]. Design principles of the air disinfection enclosures are unclear and will be established through the study.

Most of the virus protection systems are designed for healthcare workers and targeting every kind of virus and bacteria simultaneously. Although the approach is fine for the medical use of the equipment, targeting all kinds of infections can prevent the portable and user-friendly design of the equipment. Some bacteria and fungi spores are more resistant to UV light, and to remove this kind of treats from the air, HEPA filters are needed besides UV light which requires larger fans to pass the air through the air filters. In this study, we target only the COVID-19 virus to reach a portable and energy-efficient reflective enclosure.

2. Calculation Method of Required Dose for the Reflective Enclosures

2.1. Required Sterilization Dose for COVID-19 Virus. The UV-C light is altering the molecular bonds of nucleic acids within the nucleus of the viruses. How much damage occurs to the virus's genetic material is related to absorbed light energy by the virus. If collimated light is used, the cross-section of the virus is determining the absorbed dose, while for the diffuse radiation condition, the total surface area of the virus should be used.

In biological studies, the effective dosage is determined by using collimated or almost directional light. The directional property of the light in the biological experiments helps to correlate the power meter readings with the applied UV-C power to the air, where they are basically equivalent. But the enclosure that is studied here is generating diffuse light, and photons are hitting from all directions to the viruses. Because of that, the relation between the applied effective power and the power meter readings from the enclosure wall should be correlated to each other.

In literature, several biological experiments are performed to determine the effectiveness of UV-C light on airborne viruses. As the results are compared from different experiments, the required dose is hard to determine. Most of the older studies are considered unreliable as the techniques are not so mature to determine the virus effectiveness, and the coronaviruses were not at the focus of those experiments. To determine the required dose for this study, the recent three studies targeting coronaviruses are taken as the baseline.

One of the studies is using 222 nm far UV-C light. Total exposure of 1.7 and 1.2 mJ/cm² inactivated 99.9% of aerosolized coronaviruses 229E and OC43, respectively [10]. As the COVID-19 virus is a coronavirus and has a similar genomic size [11–13], UV-C light would be expected to show similar inactivation efficiency against SARS-CoV-2 (COVID-19). In our design, 254 nm light is used, and it is



FIGURE 1: UV-C air sterilization device concept [6].

expected to give similar or better inactivation based on the absorption spectrum of RNA molecules.

In the second study, aerosolized coronaviruses are exposed to 254 nm UV-C light, and 88% of the viruses were inactivated with only 0.6 mJ/cm² UV-C exposure [14]. This study is showing that coronaviruses are very sensitive to UV-C light and also in line with the results of the study explained in the first study.

In the third study, SARS-CoV-2 samples with different virus concentration levels are exposed to UV-C light. A UV-C dose of just 3.7 mJ/cm² achieved more than 3-log inactivation without any sign of viral replication for the concentrations that can be encountered in hospital rooms [15].

By considering the recent studies, 2.0 mJ/cm² dose level is decided to be the threshold dose that should be applied to the air by the portable air-sterilizing enclosure. As a result of this design decision, it is expected to reach 99.9% reduction of the infectivity of the SARS-CoV-2 coronavirus (COVID-19), which is the level that far exceeds the performance of the N95 medical masks.

2.2. Obtaining Dosage from Optical Simulations and Factor of 4x. Collimated light is used for the biological studies, while the dominant irradiance for the enclosure is diffuse illumination as shown in Figure 2. If the light is assumed to be uniform from all directions, the applied power to the airborne particles can be analytically correlated with the power meter ratings from the enclosure wall. For such a diffuse illumination, if we assume a spherical geometry object that represents the virus, the absorbed radiation will be correlated to its outer skin area, which can be calculated by $4\pi r^2$. For the collimated light, only the cross-section of the sphere

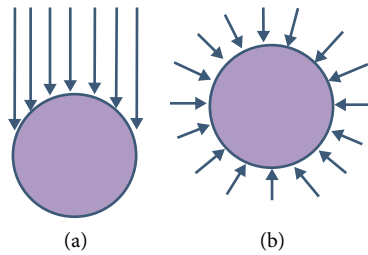


FIGURE 2: Collimated (a) vs. diffuse light (b) on a spherical particle.

should be considered, and the effective area is equal to the πr^2 . Therefore, assuming the same irradiance level is measured with the probe sensor, the applied power to the air by the diffuse illumination is 4 times the measured value by the probe sensor.

For real enclosures, the illumination is not totally diffuse. Therefore, optical simulations are necessary to correlate the probe sensor readings with the average irradiance falling on the spherical virus surface. For the calculation of the applied UV-C power, a spherical volume detector is used within the Zemax simulation. This spherical detector is showing the rays hitting its surface and giving the total power. For the applied dose calculations, the average illumination on the sphere is necessary, which can be obtained by the division of the total power reached to the spherical detector to the area of the spherical detector object. Then, the applied power will be 4 times the average irradiance on the spherical detector surface. To get the correct dosage, it is better to move the spherical detector from the inlet to the outlet of the enclosure and get the averaging, so that nonuniformity through the enclosure is included in the calculations.

Applied UV-C dose is related to how much energy is absorbed by the viruses. Therefore, the applied power should be multiplied by the exposure duration to obtain the effective dose. The diameter and length of the enclosure should be determined to supply enough airflow time and enough dosage. For the nonideal illumination case, the minimum applied power should be expected at the enclosure wall as the enclosure wall is the furthest region from the lamp. Therefore, spherical detectors should be placed as close as to the enclosure wall to ensure that the minimum required dose is applied to the flowing air.

3. Simulation of the Disinfecting Enclosure

3.1. Lamp Model Implementation and Lamp Power Measurements. In the simulations, a cylindrical volume is used to represent the tube light. The light is originating from the light source, reflects several times, and is then absorbed. Air is flowing through the reflective enclosure around the tube light for disinfection.

To get a realistic outcome from the optical simulations, initially, the light source is simulated with the optical simulation software, and the illumination behavior is confirmed with real measurements. Although the power of the lamps is generally measured by an integrating sphere, a more practical way is defined by Keitz for the tubular light source

measurements [16, 17]. In the Keitz formulation (1), E is the measured irradiance (W/m^2), D is the distance (m) from lamp center to the UV sensor, L is the lamp length (m) between electrodes, α is the half-angle (radians) subtended by the lamp at the sensor position, and P is the power (W) of the lamp.

$$P = \frac{E2\pi^2DL}{2\alpha + \sin 2\alpha} \quad (1)$$

The custom-made cold cathode tube light is selected as the light source, as shown in Figure 3. The irradiance generated by the light source is measured from different distances, and the power of the lamp is calculated by Keitz formulation for all configurations as given in Table 1. The calculated power is $0.140 \text{ W} \pm 0.002 \text{ W}$ and validated by several measurements from different distances as shown in table. The lamp has been measured by two different UV-C power meters to improve the measurement accuracy. Calculations are validated with the view factor method [1], and very identical results are obtained.

5 V is supplied to the ballast circuitry, and power consumption is measured. The electrical consumption of the lamp is 2.7 W, including the ballast circuitry. The total UV power of the lamp at steady-state condition derived from the irradiance measurements (140 mW) is leading to an efficiency of 5.2%, where efficiency is defined as the ratio of the total generated UV-C light power to the total consumed electrical power. Although the efficiency of the lamp is low compared with the large hot cathode lamps (30%), the value is still superior to the accessible UV-C LED technology (2.5%). The efficiency value makes these cold cathode lamps more suitable for this study than the current UV-C LED technology as the power consumption is critical for portable applications to reduce the battery size. More powerful lamps with similar lengths are also available with cold cathode technology. If the light levels with the selected tube light do not satisfy the required disinfection UV-C dose, the design process can be repeated with more powerful UV-C cold cathode light sources.

The equivalent configurations to the measurements are also created in Zemax (OpticStudio) environment. The light source is simulated with a power of 0.140 W. The length of the lamp is 120 mm, while the distance between the cathodes is 83 mm. Therefore, the light source used in the simulations has a length of 83 mm. Nearly, the same irradiance levels are obtained from the simulations for different distances as given in Table 2. The small differences (<2%) between the

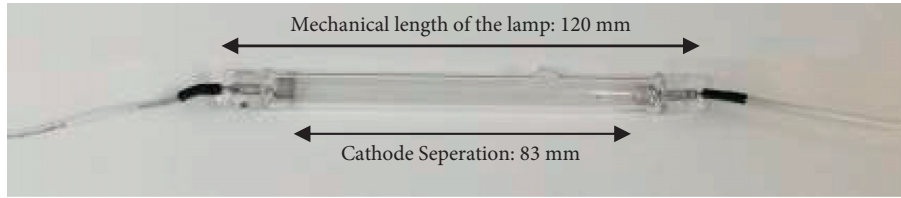


FIGURE 3: Custom-made cold cathode tube light.

TABLE 1: Lamp irradiance measurements from different distances and power calculations based on Keitz formulation.

Distance (mm)	Irradiance ($\mu\text{W}/\text{cm}^2$)	Total power (W)	Efficiency (%)
100	128.0	0.140	5.19
150	59.0	0.138	5.11
200	34.0	0.140	5.19
300	15.5	0.140	5.19

TABLE 2: Comparison of optical simulations with the measurements.

Distance (mm)	Irradiance "measured" ($\mu\text{W}/\text{cm}^2$)	Irradiance "optical simulation" ($\mu\text{W}/\text{cm}^2$)	Difference (%)
100	128.0	127.4	0.5
150	59.0	59.1	0.2
200	34.0	34.0	0.0
300	15.5	15.2	1.9

measurements and simulations can source from the non-uniform response of the sensor for the closer cases as the light rays reach to the sensor with a higher incidence angle. For the long-distance measurements, the sensitivity of the UV-C meter starts to become an issue as the irradiance reaching the sensor is very low. As the measurements and simulations are pleasantly supported by each other, the same lamp geometry and light source parameters are used confidently for the successive enclosure simulations.

3.2. Enclosure Geometry. The cylindrical shape is selected as the enclosure geometry, and an I-shape lamp is placed along the centerline of the cylindrical enclosure. This configuration will provide uniform radial illumination at the enclosure wall as a result of symmetry. The two sides of the enclosure are covered with light baffles, and there are symmetrical openings on the baffles to permit airflow.

The inward-facing surface of the first light baffle is polished aluminum with specular reflection characteristics. The other baffles in the device are made from steel and completely sandblasted to prevent harmful light leakage from the device. Experimentally validated that subsequent absorptive baffles have no detectable effect on the internal light intensity as the light returning to the enclosure from the absorptive baffles is negligible. Therefore, only the first two baffles are used, and subsequent baffles are excluded from the simulations to simplify the simulation geometry. The parts of the manufactured enclosure are shown in Figure 4.

Enclosure dimensions are affecting the light intensity reaching the enclosure wall. If the diameter of the enclosure increases, the light intensity will drop as the distance from the lamp is increased, and the light will spread to a larger surface area. But this intensity reduction at the enclosure



FIGURE 4: Parts of the manufactured enclosure.

wall does not reduce the applied dose. Increasing the enclosure diameter is slowing down the airflow by increasing the flow cross-section, and consequently, UV-C exposure duration of the air increases. Intensity at the enclosure wall decreases linearly with the diameter of the enclosure, while the duration is increased with the square of the enclosure diameter. Although this geometrical relation promotes large enclosures for energy efficiency, increasing the enclosure diameter will cause bulky devices. The limiting factor to the diameter is imposed by the size of other required sub-components such as fan and battery as shown in Figure 5.

As optical simulations do not impose a diameter limit, the enclosure diameter in this study is decided by considering the available centrifugal fans that can supply at least 30 lt/min airflow with sufficient pressure. Axial fans are also considered, but the pressure generated by small axial fans is not enough to force the air through the dust filter at the inlet of the enclosure. By comparing the off-the-shelf fans, 50 mm diameter centrifugal fans are decided to be used in this study. These fans are available from different vendors; they are very well optimized, compact, and can supply the required airflow with air filters. Making the enclosure smaller than the



FIGURE 5: Parts of the device that are used with the enclosure.

fan diameter seems not logical, as the main size determining parameter becomes the fan diameter. Therefore, the external diameter of the enclosure is selected to be 50 mm for the simulations. The thickness of the metal tube is 0.75 mm, and the internal diameter of the enclosure is 48.5 mm. The limiting minimum exposure time is also satisfied by design as it is suggested to be larger than 0.25 s [1] in literature. There can be time-dependent chemical and biological mechanisms that will change the effectiveness of the UV-C light if the exposure time is reduced. The limit can be reduced or eliminated with further biological experimental studies, but the biological studies related to the time dependency of UV-C exposure are not accessible or do not exist yet. Therefore, exposure duration larger than 0.25 s is taken as a requirement in this study and satisfied with the design parameters as given in Table 3.

3.3. Enclosure Material Selection. A portable UV-C disinfection system should be compact and must have a low power consumption. To reduce the power consumption of the lamp, the reflectivity of the internal surfaces of the enclosure should be as high as possible, so that the illumination level in the enclosure can be increased without increasing the lamp power. Aluminum, steel, and micro-porous PTFE materials are evaluated to build trustable and cost-effective enclosures.

Reflective characteristics of the enclosures are given in Table 4. Shiny internal surfaces for the metallic parts are achieved via mechanical polishing. For the PTFE material, the data from the manufacturer are used (Porex). Aluminum and steel are assumed to have totally specular reflection characteristics, while PTFE material is taken as a diffuse material with a Lambertian characteristic.

The enclosures are produced from different materials as shown in Figure 6, and the light level is measured at the enclosure wall. The measurement results are given in Table 5, including the measurement of the bare lamp from the same distance. All enclosures are increasing the irradiance levels,

TABLE 3: Design parameters of the UV-C device.

Lamp diameter	9 mm
Enclosure internal diameter	48.5 mm
Airflow cross-section	1784 mm ²
Enclosure internal length	120 mm
Flow rate	30 lt/min
Minimum exposure time	0.43 s (>0.25 s)
Minimum required dose level	2.0 mJ/cm ²

as given in Table 5. The steel enclosure only increased the power by 39%, which confirms that steel does not have good reflectivity at the UV-C spectrum. Aluminum increased the power 2.44x, while the best behavior is obtained from the PTFE material which gives an escalation of 5.01x.

By evaluating the experiments, steel is abandoned as it is not helping much to increase the illumination at the enclosure wall. In the experiments performed with the PTFE material, some kind of disturbing odor is encountered. Air quality testing is performed; but unfortunately, the root cause of the smell cannot be accurately determined. Because the user of the device will continuously breathe the air coming from the enclosure, PTFE material is avoided until more safety testing is performed and until the root cause of the odor is exactly determined. By eliminating the two possible candidates, aluminum is selected as the enclosure material.

3.4. Light Intensity near the Enclosure Wall. As the aluminum is selected to be the enclosure material, more detailed simulations and measurements are performed with an aluminum enclosure to obtain the intensity distribution along its length close to the cylindrical wall. Calibrated UV-C probe is used for the measurement of the UV radiation at the enclosure wall. The probe has a diffuser on the tip, ensuring good responsivity across all angles.

While performing enclosure simulations, the end portion of the lamp should also be correctly added to the optical model as the end portions of the lamp interact with the

TABLE 4: Enclosure materials and their reflectivity.

	Reflection type	Reflectivity (reported by the manufacturer) (%)
Aluminum	Specular (mirror-like)	70
Steel	Specular (mirror-like)	30
Microporous PTFE	Diffuse (Lambertian)	93

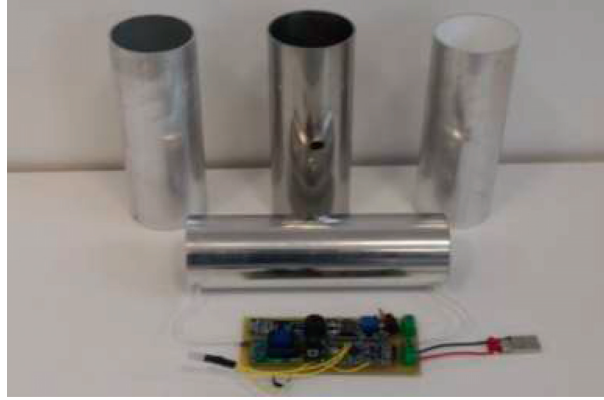


FIGURE 6: Manufactured enclosures aluminum (left), steel (middle), and PTFE (right). One of the assembled enclosures is also shown with the control electronics in the front.

TABLE 5: Irradiance measurements at the enclosure wall for different enclosure materials.

	Irradiance at enclosure wall ($\mu\text{W}/\text{cm}^2$)	Irradiance without enclosure ($\mu\text{W}/\text{cm}^2$)	Improvement
Aluminum	2528	1040	2.44x
Steel	1450	1040	0.39x
PTFE	5210	1040	5.01x

bounced light within the enclosure. The lamp sides have absorptive characteristics and decrease the light level at the end portions of the enclosure.

The enclosure has 8 mm diameter holes, and these holes are used for the probe measurement. The simulated value was $2.51 \text{ mW}/\text{cm}^2$ for the central hole, while the measured value is $2.53 \text{ mW}/\text{cm}^2$. The measurement and simulated results are strongly correlating with each other, which is showing the successful construction of the optical model for the simulations.

To consider the nonuniformity through the enclosure, we performed measurements from different points on the enclosure and compared the measurements with the simulations. To perform the measurements, a series of holes are used on the enclosure wall. While performing measurements, unused holes are covered with an aluminum sheet to prevent leakage from the holes. As predicted by the simulations, the irradiance diminishes from the center to the edges, as shown in Figure 7.

Within the simulations, the lamp is assumed to have uniform irradiance through its length, but in reality, the lamp irradiance distribution is not uniform through the lamp axis. As a result, the simulated and measured intensity distribution is slightly different through the enclosure. The average irradiance through the enclosure is $1954 \mu\text{W}/\text{cm}^2$, obtained by the measurements; while from the simulations, it is obtained to be $1944 \mu\text{W}/\text{cm}^2$. The values have less than

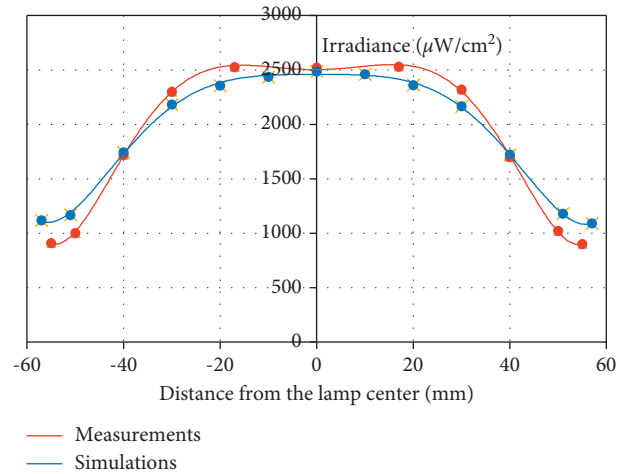


FIGURE 7: Irradiance measurements from the enclosure wall through the length of the enclosure.

1% difference, and for the remaining dose calculations, the optical model can be used safely.

The dose calculation requires a spherical detector within the simulations. At several points, through the enclosure, the irradiance on a spherical sensor is obtained as shown in Figure 8. The average intensity distribution can be used for the dose calculations as the flow is uniform across the enclosure.

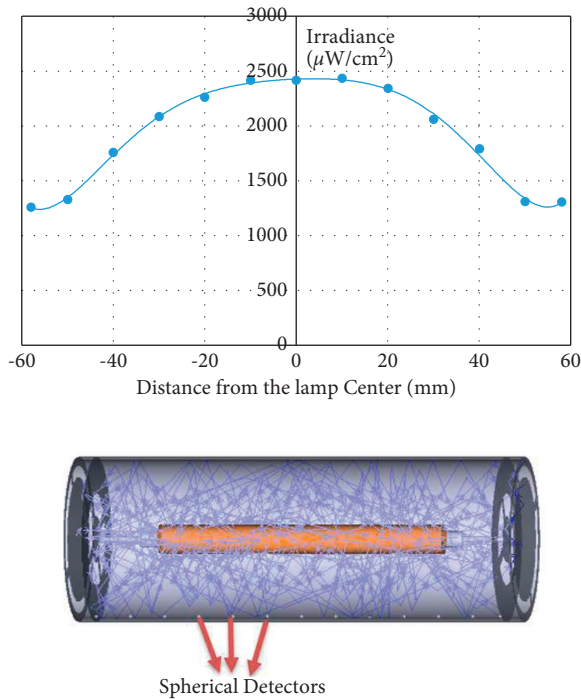


FIGURE 8: Average irradiance measurements with a spherical detector through the enclosure.



FIGURE 9: Produced UV-C air sterilization device.

To obtain the average intensity value through the enclosure, a 6th-order polynomial curve is generated from the known data points, and the average value of the function is calculated through the enclosure. The average irradiance inside the enclosure falling on a spherical particle is obtained to be $1953 \mu\text{W}/\text{cm}^2$.

4. Realization of a Portable UV Sterilization Device with the Enclosure

The last step of the calculations is the estimation of the applied UV-C dose. Dose estimation is achieved by the multiplication of the duration (0.43 s) with the average irradiance on a spherical particle ($1953 \mu\text{W}/\text{cm}^2$) and with the spherical form factor (4.0) as introduced in Section 2.2. By multiplying the terms, the dose applied by the enclosure is obtained as $3.36 \text{ mJ}/\text{cm}^2$, which is higher than the minimum required value, $2.0 \text{ mJ}/\text{cm}^2$. With this dose level, the enclosure can securely disinfect the air for the user.

A portable device that is attachable to the belt is also designed using the enclosure explained in this study, and the produced device is shown in Figure 9.

The sterilization level of the enclosure is also validated by biological tests. The airborne COVID-19 viruses are given to the device, and the effectiveness of the device is reported to be better than 99.5% by the accredited test laboratory of "Anti-Microbe Biocidal Analyses Center" in Ankara. The test result confirms the effectiveness of the UV-C enclosure device against the COVID-19 virus.

5. Conclusion

In this study, design principles of the air-sterilizing UV-C reflective enclosures are established, and a portable device is successfully developed. Small, portable, and power-efficient enclosures can supply the required UV-C dosage and exposure duration to kill the viruses in the inhaled air. Radiation characteristic through the enclosure is measured, and applied dose is obtained by merging measurements with the optical simulations. Direct measurement of the UV-C light level from the enclosure wall is not equivalent to the power applied to the air. To correlate measurements with the effective dose, the cumulative effect on a unit air volume should be calculated. The light levels at the representative points are averaged to reach the total irradiance applied to the air through the enclosure. As the enclosure illuminates the virus particles from all directions, a multiplication factor of 4 is required. A portable UV-C air sterilization device is also developed based on the reflective enclosure reported in this study. The developed device is tested against the virus of the current pandemic (COVID-19), and disinfection effectiveness (>99.5%) of the reflective enclosure is demonstrated. Because of the mutations, vaccines generally lose their effectiveness against viruses. UV-C air sterilization systems based on reflective enclosures can help fight against the mutated viruses until new vaccines are developed.

Data Availability

The irradiance measurement data used to support the findings of this study are included within the article.

Conflicts of Interest

The author declares that there are no conflicts of interest.

References

- [1] W. Kowalski, *Ultraviolet Germicidal Irradiation Handbook: UVGI for Air and Surface Disinfection*, Springer, Berlin, Germany, 2009.
- [2] C. S. Rosemary, D. Chen, P. Pak, D. K. Armani, A. Schubert, and A. M. Armani, "Lightweight UV-C disinfection system," *Biomedical Optics Express*, vol. 11, pp. 4326–4332, 2020.
- [3] A. M. Armani, D. E. Hurt, D. Hwang, M. C. McCarthy, and A. Scholtz, "Low-tech solutions for the COVID-19 supply chain crisis," *Nature Reviews Materials*, vol. 5, no. 6, pp. 403–406, 2020.
- [4] M. Purschke, M. Elsamaloty, J. P. Wilde et al., "Construction and validation of UV-C decontamination cabinets for filtering

- facepiece respirators,” *Applied Optics*, vol. 59, pp. 7585–7595, 2020.
- [5] J. P. Wilde, T. M. Baer, and L. Hesselink, “Modeling UV-C irradiation chambers for mask decontamination using zemax OpticStudio,” *Applied Optics*, vol. 59, no. 25, pp. 7596–7605, 2020.
- [6] N. Mahanta, V. Saxena, L. M. Pandey, P. Batra, and U. S. Dixit, “Performance study of a sterilization box using a combination of heat and ultraviolet light irradiation for the prevention of COVID-19,” *Environmental Research*, vol. 198, Article ID 111309, 2021.
- [7] L. G. Leanse, C. Dos Anjos, J. F. Besegato, T. Dai, and A. N. S. Rastelli, “Shedding UVC light on Covid-19 to protect dentistry staff and patients,” *Laser Physics Letters*, vol. 18, no. 8, Article ID 085602, 2021.
- [8] M. Bormann, M. Alt, L. Schipper et al., “Disinfection of SARS-CoV-2 contaminated surfaces of personal items with UVC-LED disinfection boxes,” *Viruses*, vol. 13, no. 4, p. 598, 2021.
- [9] M. R. Ricci, *Ultra-Violet Germicidal Mask System*, US Patent, Alexandria, VA, USA, 1992.
- [10] M. Buonanno, D. Welch, I. Shuryak, and D. J. Brenner, “Far-UVC light (222 nm) efficiently and safely inactivates airborne human coronaviruses,” *Scientific Reports*, vol. 10, no. 1, p. 10285, 2020.
- [11] A. R. Fehr and S. Perlman, “Coronaviruses: an overview of their replication and pathogenesis,” in *Coronaviruses: Methods and Protocols*, H. J. Maier, E. Bickerton, and P. Britton, Eds., pp. 1–23, Springer New York, Berlin, Germany, 2015.
- [12] B. W. Neuman, B. D. Adair, C. Yoshioka et al., “Supramolecular architecture of severe acute respiratory syndrome coronavirus revealed by electron cryomicroscopy,” *Journal of Virology*, vol. 80, no. 16, pp. 7918–7928, 2006.
- [13] U. Celik, K. Celik, S. Celik et al., “Interpretation of SARS-CoV-2 behaviour on different substrates and denaturation of virions using ethanol: an atomic force microscopy study,” *RSC Advances*, vol. 10, no. 72, pp. 44079–44086, 2020.
- [14] C. M. Walker and G. Ko, “Effect of ultraviolet germicidal irradiation on viral aerosols,” *Environmental Science & Technology*, vol. 41, no. 15, pp. 5460–5465, 2007.
- [15] M. Biasin, A. Bianco, G. Pareschi et al., “UV-C irradiation is highly effective in inactivating SARS-CoV-2 replication,” *Scientific Reports*, vol. 11, no. 1, p. 6260, 2021.
- [16] H. A. E. Keitz, “Non-point sources,” in *Light Calculations and Measurements: An Introduction to the System of Quantities and Units in Light-Technology and to Photometry*, H. A. E. Keitz, Ed., pp. 115–145, Macmillan Education, London, UK, 1971.
- [17] M. Sasges, J. Robinson, and F. Daynouri, “Ultraviolet lamp output measurement: a concise derivation of the keitz equation,” *Ozone: Science & Engineering*, vol. 34, no. 4, pp. 306–309, 2012.